EFDA–JET–CP(10)03/10

M. Gatu Johnson, E. Andersson Sundén, M. Cecconello, S. Conroy, G. Ericsson, J. Eriksson, G. Gorini, C. Hellesen, V. Kiptily, M. Nocente, S. Sangaroon, S.E. Sharapov, M. Tardocchi, D. van Eester, M. Weiszflog and JET EFDA contributors

Neutron Spectrometry of JET Discharges with ICRH-Acceleration of Helium Beam Ions

Neutron Spectrometry of JET Discharges with ICRH-Acceleration of Helium Beam Ions

M. Gatu Johnson[1], E. Andersson Sundén[1], M. Cecconello[1], S. Conroy[1], G. Ericsson[1], J. Eriksson[1], G. Gorini[2], C. Hellesen[1], V. Kiptily[3], M. Nocente[2], S. Sangaroon[1], S.E. Sharapov[3], M. Tardocchi[2], D. van Eester[4], M. Weiszflog[1] and JET EFDA contributors*

JET-EFDA, Culham Science Centre, OX14 3DB, Abingdon, UK

[1]Department of Physics and Astronomy, Uppsala University, Box 516, SE-75120 Uppsala, Sweden (EURATOM-VR)
[2]Physics Department, Milano-Bicocca University, and Istituto di Fisica del Plasma del CNR, Milan, Italy (EURATOM-ENEA-CNR)
[3]EURATOM-UKAEA Fusion Association, Culham Science Centre, OX14 3DB, Abingdon, OXON, UK
[4]LPP-ERM/KMS, Association Euratom-'Belgian State', TEC Partner, Brussels, Belgium
** See annex of F. Romanelli et al, "Overview of JET Results", (Proc. 22 [nd] IAEA Fusion Energy Conference, Geneva, Switzerland (2008)).*

Preprint of Paper to be submitted for publication in Proceedings of the 18th High Temperature Plasma Diagnostics, Wildwood, New Jersey, USA. (16th May 2010 - 20th May 2010)

ABSTRACT

Recent experiments at JET aimed at producing ^{4}He ions in the MeV range through 3rd harmonic ICRH acceleration of ^{4}He beams in a ^{4}He plasma. MeV range D was also present through parasitic ICRH absorption on residual D. In this contribution, we analyze TOFOR neutron spectrometer data from these experiments. A consistent description of the data is obtained with d(d,n)^{3}He and ^{9}Be(α,n)^{12}C neutron components calculated using Stix distributions for the fast D and ^{4}He, taking finite Larmor radius effects into account and with a ICRH power partition of $P_D^{RF} = 0.01 \times P_{4He}^{RF}$, in agreement with TOMCAT simulations.

1. INTRODUCTION

Recent JET experiments were aimed at production of energetic helium ions in the MeV energy range with 3rd harmonic ICRH-acceleration of ^{4}He beam ions, to mimic fusion-born alpha particles. This technique permits the experimental investigation of the MeV energy helium ions mimicking fusion-born alpha particles without the complications of a DT campaign. The scenario is complicated by a residual minority of D in the vessel, absorbing the ICRH power at the same frequency as 4He, similar to the experiments described in [1,2,3]. Populations of fast ^{4}He and D will hence be present in the plasma.

Data was collected during a series of 8 successful pulses, with magnetic field B_T=2.25T, applied ICRH frequency $\omega_{RF} = 51.4$MHz, average electron density $n_e = 2.8\times10^{19}\ m^{-3}$ (varying in the range 2.5-4$\times10^{19}\ m^{-3}$), electron temperature $T_e = 3.4$keV (from high resolution Thomson scattering), D density $n_d = 0.158\times n_e$ and ^{4}He density $n_{^4He} = 0.385\times n_e$ (deduced from light spectroscopy and Z_{eff} measurements). ^{9}Be was seeded to the plasma with estimated density $n_{Be} = 0.005\times n_e$. Typical neutron rates (R_{NT}), NB and ICRH powers (P_{NB} and P_{RF}) for the experiment are shown in Fig.1, where the traces at early times show the time evolution for Pulse No: 79174 and those at later times represent Pulse No: 79170. It should be noted that the NB power is doubled for Pulse No: 79174 with two ^{4}He Positive Ion Neutral Injectors (PINIs) applied, compared to Pulse No: 79170 with single PINI ^{4}He NB heating. Note also the slow build-up of the neutron rate, indicating a slow ICRH tail formation process.

The neutron emission during this experiment was observed using the TOFOR neutron spectrometer4, located in the JET roof laboratory with a vertical view through the plasma core. The Line-Of-Sight (LOS) of TOFOR is described in detail in [5]. It is approximately limited to the range 2.74–3.02m at the torus midplane (R_{maj} JET = 2.96m). The instrument consists of two sets of plastic scintillators at a distance of about 1.2m from each other; the neutron energy is deduced from the measured time-of-flight between the two detector sets. The full response of the system to incident neutrons has been simulated using GEANT4 in the range $E_n = 1-18$MeV and is used in the analysis of TOFOR data. To lowest order, $E_n = (1.02\times10^2/t_{TOF})2$; this means that the 2.45MeV neutrons from thermonuclear d(d,n)3He reactions show up as a peak around 65ns in the spectrum.

A neutron spectrum from similar experiments run at JET in 2004, obtained from Minimum

Fisher Regularization unfolding of NE213 data, is shown in [6]. The authors claim the observation of a $E_n = 2.45$MeV neutron peak from d(d,n)^{3}He reactions, and a number of higher energy peaks that they expect to originate from ^{9}Be(α,n)^{12}C reactions. No qualitative estimate of how the different ion distributions manifest themselves in the data is given. Neutron spectra from ^{9}Be(^{3}He,n)^{11}C reactions have been recently measured at JET, as reported in [7], where the cross sections and neutron spectra for the ^{9}Be(α,n)^{12}C reaction were also established.

In this contribution, we analyze the measured neutron spectra from the experiment using Monte Carlo calculated d(d,n)^{3}He and ^{9}Be(α,n)^{12}C neutron components and interpret the results in terms of the underlying physics. We conclude that a consistent description of the data is obtained using Stix distributions for ^{4}He and D, with an ICRH power partition in agreement with TOMCAT [8] simulations, and taking finite Larmor radius effects into account.

2. DATA ANALYSIS

The D and ^{4}He ion distributions in the plasma center [Fig.2] have been calculated using the Stix formalism [9] with a full treatment of the ICRH diffusion coefficient and with average experimental parameters as input. Especially noteworthy is the sharp cut-off in the distribution function at an energy E^*, approximately proportional to B^2/n_e as discussed in [10].

Figure 3 shows the summed TOFOR data collected during all 8 pulses of the experiment (Pulse No's: 79167-79175, excluding 79172). A feature of interest is the absence of a peak in the region 60-70ns, i.e., no regular thermonuclear d(d,n)^{3}He peak is observed. There is a clear cut-off around 42ns in the data, consistent with the reproduction of the D distribution E^* in the neutron spectrum, as previously observed for 3rd harmonic ICRH tuned to D beams in D plasmas at JET.11 There is also a significant number of neutrons observed above E* in energy, i.e., in the region $30 < t_{TOF} <$ 40ns. These originate from ^{9}Be(α,n)^{12}C reactions.

The data has been analyzed with the help of model components on a neutron energy scale. In Fig.3(a), d(d,n)^{3}He and ^{9}Be(α,n)^{12}C components, folded with the TOFOR response function, are shown together with the data. These components are calculated with the Monte Carlo code ControlRoom [12], sampling from the Stix 4He distribution and a Maxwellian 3.4-keV Be distribution and from the Stix D distribution reacting with itself, respectively. In the component calculation, the total applied ICRH power ($P_{RF} = 4.34$MW on average for the session) has been divided between the D and ^{4}He species until the intensity ratio between the $t_{TOF} < 40$ns and $t_{TOF} > 40$ns regions of the spectrum was reproduced. The components in Fig.3(a) are not fitted to the data; their intensity has been scaled to approximately match the measurement. We find that the intensity ratio ^{9}Be(α,n)^{12}C to d(d,n)^{3}He is reproduced if $P_{RF}^{D} \approx 0.01 \times P_{RF}^{4He}$.

This result was compared with simulations of the ICRH wave absorption properties of the scenario using the 1D wave code TOMCAT (Fig.4). TOMCAT assumes Maxwellian distributions for all species involved; the beam ^{4}He distribution is approximated as a $T_{4He} = 50$keV Maxwellian. The temperature of all other species is set to $T = T_e = 3.4$keV. Realistic values for the densities are used.

TOMCAT gives a total absorption efficiency for the scenario of 30.3%, with 16.3% of the power absorbed by the ^{4}He beam population, 0.18% by the residual D and 13.6% by the electrons. The TOFOR observation of $P_{RF}^{D} \approx 0.01 \times P_{RF}^{4He}$ is in agreement with the TOMCAT result.

The components from Fig.3(a) are shown on a neutron energy scale in Fig.5(a), where also the ^{9}Be(d,n)^{10}B simulation result is shown. The multiple peaks in the ^{9}Be(α,n)^{12}C and ^{9}Be(d,n)^{10}B cases represent excited states of the product nucleus.

The components are shown on an absolute scale ($m^{-3}MeV^{-1}s^{-1}$) as obtained from the calculations. It is clear that any ^{9}Be(d,n)^{10}B contribution will be below the observable level in the data.

As can be seen in Fig.3(a), the calculated d(d,n)^{3}He component is not a satisfactory description of the data on the low neutron energy side ($t_{TOF} > 60$ns). This can be understood as a consequence of the finite Larmor radius for high energy ions.

With the ICRH resonance centered at 3.05m and the line-of-sight at the torus mid-plane covering the region 2.74–3.02m, it is clear that the downward motion of a significant fraction of ion orbits will fall outside of the LOS, while the upward motion will fall inside. The neutron energy (E_n) spectrum is kinematically broadened due to the high reactant energies, with the upward motion leading to high E_n as observable from above, and the downward motion to low E_n. This means that with the downward motion falling outside of the instrument LOS, low energy neutrons will be lost. This is taken into account in the analysis as presented in Fig.3(b). Here, the dashed components from Fig.5(b) are used to describe the d(d,n)^{3}He and ^{9}Be(α,n)^{12}C neutrons.

These components are calculated with a new Monte Carlo code [13] taking the line-of-sight effect into account. In the calculation, the fast ion distributions are assumed to be those obtained from Stix within a limited radial interval. The interval is obtained as the full width at half maximum of a Gaussian fit to the TOMCAT [4] Hebeam absorption curve from Fig.4, i.e., R = 2.91–3.11m. In Fig.5(b), the spectra taking the LOS into account (dashed lines) are shown together with the full E_n spectra (solid lines); the full spectra calculated using the new code are seen to match the results from the ControlRoom calculation.

The components taking the LOS effect into account are fitted to the data in Fig.3(b). A component due to scattered neutrons is also used in the fit. The shape and intensity (0.167×direct) of this component is fixed relative to the direct E_n spectrum according to MCNPX simulation results. [5] The neutron spectrum resulting from the fit (with $C_{red} = 1.16$) is shown in Fig.6, where the d(d,n)^{3}He, ^{9}Be(α,n)^{12}C and scatter components are also indicated. Neutrons from ^{9}Be(α,n)^{12}C reactions are observed with relative intensity $N_{\alpha Be}/(N_{DD} + N_{\alpha Be}) = 0.33$. A value $n_e = 2.6\times10^{19}$ m^{-3} yields a good fit to the data in terms of E*. The measured data are consistent with the presence of deuterons with $E_D < 2.5$MeV and ^{4}He with $E_{^4He} < 5.5$MeV. This spectrum can be compared to the result for Pulse No: 62955 from the 2004 experiment.6 The authors show only the spectrum for $E_n < 7$ MeV. The peak at $E_n = 5$MeV is likely to represent E* from the D distribution. This is lower than the E* observed in our case, consistent with a higher $n_e = 2.6\times10^{19}$ m^{-3} for Pulse No: 62955.

The statistics in the TOFOR data from the pulses studied in this experiment are too low for

sepa*r*ate study of individual pulses. Separate analysis of data from periods of single and double PINI NB heating has been tried. This shows that 4He heating dominates in the single PINI case ($P_{RF}^{D} \approx 0.005 \times P_{RF}^{4He}$), while D heating becomes more important in the double PINI case ($P_{RF}^{D} \approx 0.02 \times P_{RF}^{4He}$). This is consistent with gamma spectroscopy observations. Fast D is diag*n*osed through measurements of the 3.09MeV gamma peak from $^{12}C(d,p)^{13}C$ reactions, fast ^{4}He through *o*bservation of the 4.44MeV gamma peak from $^{9}Be(\alpha,n)^{12}C$ reactions [14]. Two different gamma spectrometers, a high purity Ge (HpGe) crystal and a LaBr scintillator [15], were used during the experiment, both placed in the TOFOR line-ofsight, about 3m further away from the JET vessel. HpGe data is available for single PINI pulses, LaBr for double PINI. The relative intensity of the 3.09 and 4.44MeV peaks for the single PINI pulses is 1.64, for double PINI 5.71, taking into account the energy dependence in the detector efficiencies. Interesting to note is that this observation is not reproduced in the TOMCAT simulations: according to these, the increased 4He beam density in the double PINI case should lead to higher relative 4He absorption. This is not understood at this point.

3. DISCUSSION

Several factors impact on the results obtained in the analysis of TOFOR data from this experiment. The ICRH power partition between D and ^{4}He and E* in especially the D distribution are factors that can be fairly well established from the TOFOR analysis. Other factors with an important impact on the results obtained are the *d*ensities of the species involved and simplifications made in the line-of-sight effect calculations.

Regarding the line-of-sight effects, it is clear that the assumption of a fixed-shape fast ion distribution over the radial interval 2.91-3.11m and bulk ions only outside of this radial interval is a rather crude estimate of the true scenario. It can however been seen [Fig.3] that an effect of the order obtained in this simple estimate is needed to describe the data. It should be stressed that if the radial interval used in the simulation is shifted towards the high-field side of the plasma, the line-of-sight effect is decreased (more downward motion orbit sections fall within the line-of-sight), while the effect is enhanced if the interval is shifted towards the high-field side. The code developed to take line-of-sight effects into account is able to take fast ion distributions from SELFO as input for a more accurate estimate – however, we have not been able to obtain any SELFO results for these pulses.

As mentioned, no clear thermonuclear $d(d,n)^{3}He$ peak can be distinguished in the TOFOR data [Fig.3]. However, the simulated components show a thermonuclear peak, which leads to a rather poor description of the data in the region $60 < t_{TOF} < 70$ns. This can be understood from looking at Figure 2; A significant fraction of the calculated D population falls at low energies consistent with a "bulk" D population. If a l*o*wer n_D was assumed, the ICRH would accelerate a larger fraction of the D population, resulting in a lower "bulk" part of the distribution and a smaller thermonuclear peak. This means that TOFOR data suggests that n_D is overestimated. In fact, we have seen also in other experiments, where "clean" $d(d,n)^{3}He$ data in the 2.45MeV peak region allow for n_D to be deduced from TOFOR data,

[16] that n_D deduced with the method used here (from visible spectroscopy, based on light measured in the divertor region) overestimates the TOFOR "c*o*re" n_D result.

CONCLUSIONS

In this p*a*per, it has been shown that measurements with the TOFOR neutron spectrometer at JET during an experiment with 3rd harmonic ICRH tuned to ^{4}He be*a*ms in bulk ^{4}He plasmas with residual D can be consistently described with simulated components calculated for D and ^{4}He ion distributions in the MeV range. Fast neutrons from $d(d,n)^3He$ and $^9Be(\alpha,n)^{12}C$ reactions are observed. Neutrons from $^9Be(d,n)^{10}B$ are also produced in this scenario but with an intensity below the observable level in the data. 33% of the total neutrons incident on TOFOR are found to originate from ^{9}Be reactions.

The relative intensity between the $d(d,n)^3He$ and $^9Be(\alpha,n)^{12}C$ neutrons is reproduced if $P_D^{RF} = 0.01 \times P_{4He}^{RF}$ is assumed, in agreement with predictions from the 1D wave code TOMCAT. TOFOR data and gamma spectroscopy measurements of pulses with single or double PINI NBI heating suggest that P_D^{RF}/P_{4He}^{RF} is higher in the double PINI case.

A line-of-sight effect that occurs due to the finite Larmor radius of the high energy ions in combination with the limited field of view of TOFOR needs to be taken into account to accurately fit the data with the simulated components on the low neutron energy side. A code has been developed that takes this effect into account in the neutron spectrum calculation, and the calculated spectra used in the fit to the data.

The E* cut-off in the fast D and ^{4}He distributions due to finite Larmor radius effects is reproduced in the measured timeof- flight spectrum. This measured E* is accurately fitted with simulated components assuming $n_e = 2.6 \times 10^{19}\ m^{-3}$, consistent with fast ion distributions with $E_D < 2.5$MeV and $E_{4He} < 5.5$MeV.

ACKNOWLEDGEMENTS

This work, supported by the European Communities under the contract of Association between EURATOM and VR, was carried out under the framework of the European Fusion Development Agreement. The views and opinions expressed herein do not necessarily reflect those of the European Commission.

REFERENCES

[1]. M.J. Mantsinen et al., Physical Review Letters **88** (2002) 105002-1 (4pp)
[2]. S. Sharapov et al., Nuclear Fusion **45** (2005) 1168
[3]. V.G. Kiptily et al., Nuclear Fusion **45** (2005) L21
[4]. M. Gatu Johnson et al., Nuclear Instruments and Methods A **591** (2008) 417-430
[5]. M. Gatu Johnson et al., Modelling and TOFOR measurements of scattered neutrons at JET, submitted to Plasma Physics Controlled Fusion, under review

[6]. J. Mlynar, J.M. Adams, L. Bertalot and S. Conroy, Fusion Engineering and Design **74** (2005) 781-786

[7]. M. Gatu Johnson et al, Nuclear Fusion **50** (2010) 045005

[8]. D. Van Eester and R. Koch, Plasma Physics Controlled Fusion **40** (1998) 1949–1975

[9]. T.H. Stix, Nuclear Fusion **15** (1975) 737-754

[10]. A. Salmi et al., Plasma Physics Controlled Fusion **48** (2006) 717–726

[11]. C. Hellesen et al., Nuclear Fusion **50** (2010) 022001 (5pp)

[12]. Ballabio L Calculation and Measurement of the Neutron Emission Spectrum due to Thermonuclear and Higher-Order Reactions in Tokamak Plasmas PhD Thesis, Acta Universitatis Upsaliensis No. 797 2003 Faculty of Science and Technology Uppsala University

[13]. J. Eriksson, Calculations of neutron energy spectra from fas*t ion re*actions in tokamak fusion plasmas, Uppsala University Diploma Thesis UPTEC F10 016, http://urn.kb.se/resolve?urn=urn:nbn:se:u*u:diva-120425*

[14]. V. Kiptily et al., Nuclear Fusion **42** (2002) 999-1007

[15]. M. Nocente et al., Energy resolution of gamma-ray spectroscopy of JET plasmas with a LaBr3 scintillator detector and digital data acquisition, these proceedings

[16]. C. Hellesen et al., Neutron spectro*scopy results of JET highperformance plasmas an*d extrapolations to DT performance, these proceedings

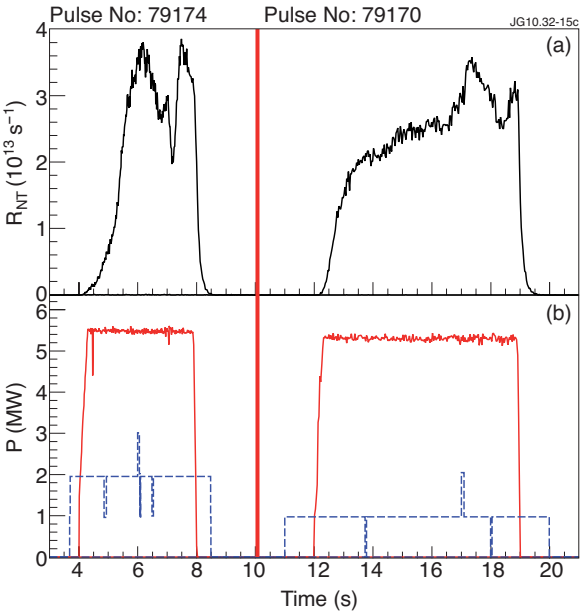

Figure 1: (a) Typical neutron rates (R_{NT}), and (b) NB (short-dashed blue) and ICRH (solid red) powers from the experiment as functions of plasma time. To the left are traces for JET Pulse No: 79174, to the right 79170.

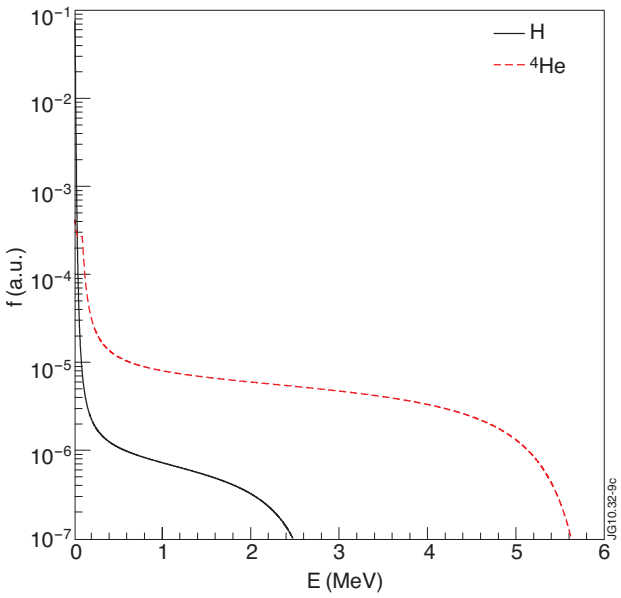

Figure 2: D (solid) and ^{4}He (dashed) ion distributions calculated using the Stix formalism with n_e = 2.6×10^{19} m^{-3} and other plasma parameters as described in the introduction.

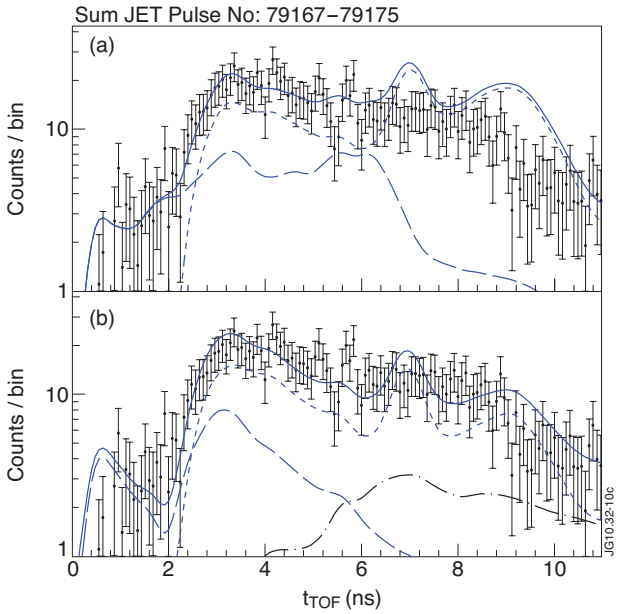

Figure 3: Summed TOFOR data from the 8 successful pulses of the experiment, (a) with ControlRoom d(d,n)^{3}He and ^{9}Be(α,n)^{12}C neutron components as discussed in the text and (b) with fitted total sum (solid), d(d,n)^{3}He (short dashed), ^{9}Be(α,n)^{12}C (long dashed) and scattered (broken) neutron components taking line-of-sight effects into account.

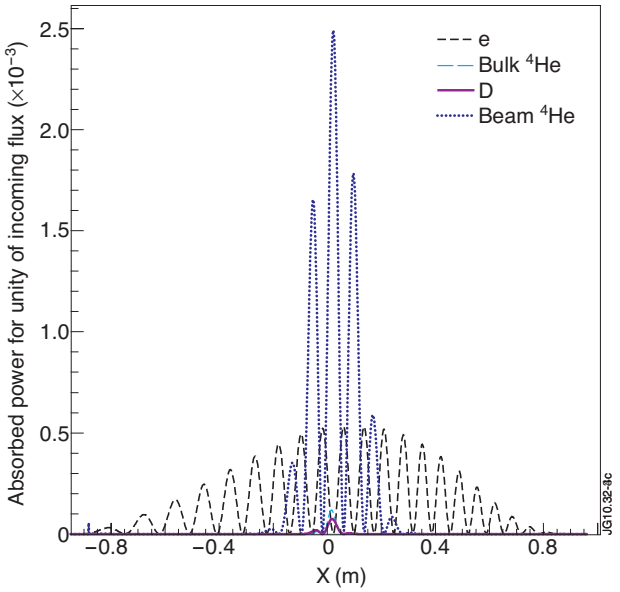

Figure 4: ICRH absorption result from TOMCAT as a function of $x = R - R_0$ ($R_0 = 2.985$m). ^{4}He beam absorption dominates.

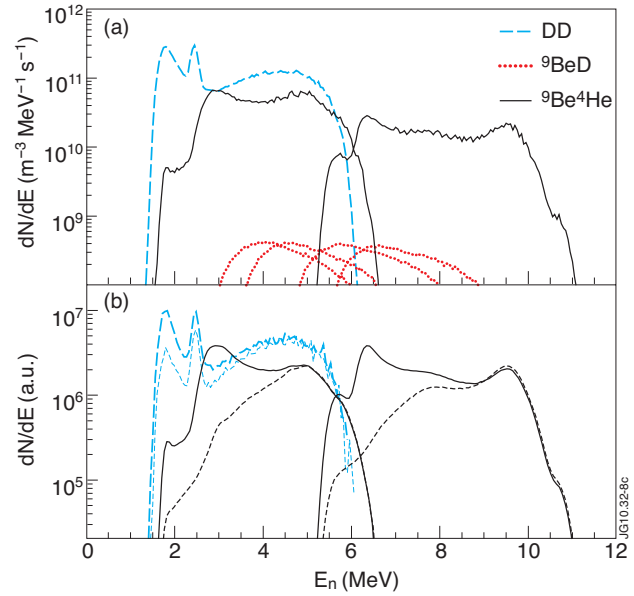

Figure 5: Neutron spectra for the d(d,n)^{3}He (long-dashed blue), ^{9}Be(α,n)^{12}C (solid magenta) and ^{9}Be(d,n)^{10}B (dotted red) reactions calculated using (a) ControlRoom and (b) a new Monte Carlo code. In (a), the intensities are determined on an absolute scale. In (b), also the spectra calculated taking the limited line-ofsight of TOFOR into account are shown (short-dashed lines).

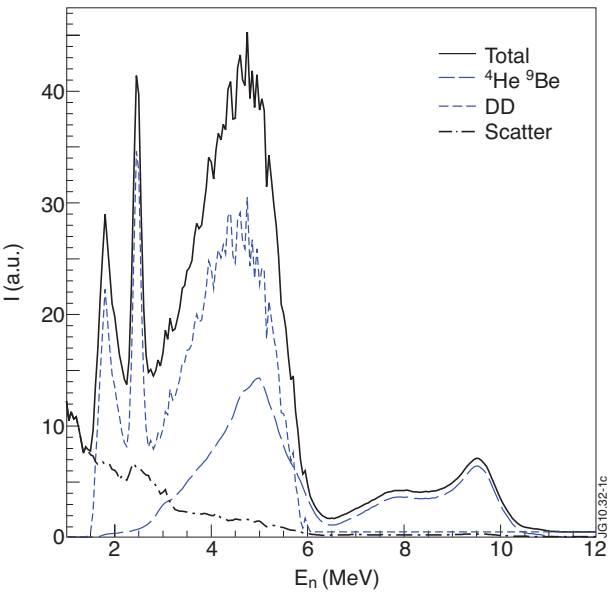

Figure 6: Total neutron spectrum (solid line) deduced from a fit to the data [Fig. 3(b)] using d(d,n)3He (short dashed), ^{9}Be(α,n)^{12}C (long dashed) and scatter (dot-dash) components.